mutations in the coding region [Rao et al., 1997; Belin et al., 1998; Shears et al., 1998; Benito-Sanz et al., 2005, 2011, 2012b; Fukami et al., 2005, 2006; Bertorelli et al., 2007; Sabherwal et al., 2007; Chen et al., 2009; Durand et al., 2010]. The putative enhancers of *SHOX* have been mapped to a ~300 kb region ~95 kb upstream, and to a ~30 kb region ~250 kb downstream from the start codon [Benito-Sanz et al., 2005, 2012a,b; Fukami et al., 2006]. The putative downstream enhancer region contains several conserved non-coding elements (CNEs) that exert enhancer activity in the developing chicken limb bud [Sabherwal et al., 2007] and in human osteosarcoma cells [Fukami et al., 2006; Benito-Sanz et al., 2012b]. Since molecular abnormalities have not been detected in a substantial portion of patients with LWD/LMD [Zinn et al., 2002; Fukami et al., 2008; Rosilio et al., 2012], it appears that unknown genetic or environmental factors are also involved in the development of these conditions.

The clinical severity of SHOX abnormalities is highly variable [Binder, 2011]. Relatively severe phenotypes in adult female patients indicate that gonadal estrogens enhance skeletal abnormalities in SHOX abnormalities [Ogata et al., 2001; Binder, 2011]. However, there may be other phenotypic modulators for this condition [Binder et al., 2004]. Here, we report on a male infant with mild LMD phenotype and compound heterozygosity of hitherto unreported microdeletions in PAR1.

CLINICAL REPORT

This Japanese male infant was a dizygotic twin conceived by in vitro fertilization. At 24 weeks gestation, an ultrasound examination delineated short extremities in one fetus and a normal skeletal appearance in the other. At 27 weeks gestation, caesarean section was performed because of bradycardia in both fetuses. At birth, the patient presented with a mesomelic appearance with a body length of 33.5 cm (–1.1 SD), weight of 1,130 g (+0.4 SD), and head circumference of 26.5 cm (+1.0 SD). His twin brother was normally proportioned with body length 35.5 cm (–0.1 SD), weight 854 g (–1.5 SD), and head circumference 25.0 cm (±0 SD). Bone survey of the patient at 2 months of age showed markedly curved radii, hypoplastic ulnas and fibulas, and metaphyseal splaying (Fig. 1A). The patient and his brother received standard medical interventions for prematurity, and were discharged from hospital at 3 months of age.

On his latest visit at 21 months of age, the infant manifested obvious mesomelic short stature with a height of 69.3 cm (−3.9 SD), weight of 8.0 kg (−2.7 SD), and head circumference of 46.6 cm (−1.0 SD; Fig. 1B). His developmental milestones were almost normal. His brother had a proportionate short stature with a height of 74.1 cm (−2.6 SD), weight of 8.5 kg (−2.3 SD), and head circumference of 46.2 cm (−1.3 SD). The mother showed limited movement of the wrist and mesomelic short stature (140 cm, −3.6 SD), while the father was clinically normal and had a normal height (165 cm, −1.0 SD). Radiological examinations were not performed for the parents or brother.

MOLECULAR ANALYSES

This study was approved by the Institutional Review Board Committee at the National Center for Child Health and Development.

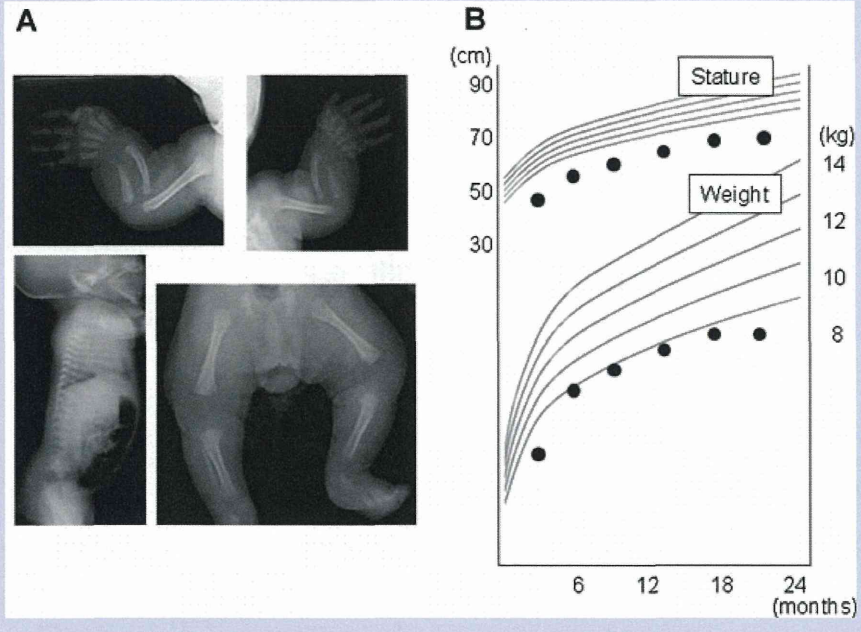

FIG. 1. Clinical findings of the infant. A: X-Ray at 10 weeks of age. Markedly curved radii, hypoplastic ulnas and fibulas, and metaphyseal splaying are shown. B: Growth pattern. Height and weight of the infant are plotted on the longitudinal height and weight standards for Japanese boys (the mean, ±1.0 SD and ±2.0 SD, respectively).

After taking written informed consent from the parents, leukocyte genomic DNA samples were obtained from the infant and parents. First, we performed direct sequencing analysis for *SHOX* by a previously described method [Shears et al., 1998]. No nucleotide alterations in the coding exons were identified in the infant. Next, we performed multiplex ligation-dependent probe amplification (MLPA) using a SALSA MLPA Kit (P018 SHOX-F1, MRC-Holland, Amsterdam, the Netherlands). Two heterozygous deletions in PAR1 were identified in the infant; a deletion involving exons 1–5 of *SHOX*, and a deletion affecting the downstream region of *SHOX* that corresponds to four MLPA probes from 05649-L20176 to 13911-L19678 (Fig. 2). Then, we examined the extent of the deletions by comparative genomic hybridization (CGH) using a custom-built oligo-microarray harboring 26,274 probes for PAR1 and several reference probes for other chromosomal regions (4 × 180 K format, Agilent Technologies, Palo Alto, CA; Fig. 3A). The telomeric deletion included a ~46 kb genomic interval (ChrX: 556,720–603,222; hg 19, Build 37) affecting *SHOX* exons 1–5 and a ~28 kb region at the 5′ side of exon 1. The centromeric deletion encompassed a ~500 kb interval (ChrX: 881,006–1,387,599) and started at a point ~300 kb from the start codon of *SHOX*. In silico analysis using UCSC Genome Browser (http://genome.ucsc.edu/) and rVista 2.0 (http://rvista.dcode.org/) revealed that the deletions did not affect the putative upstream or downstream enhancer regions of *SHOX*, and that the downstream deletion encompassed a gene for cytokine receptor-like factor 2 (*CRLF2*) and several CNEs (Fig. 4). Most of these CNEs were well conserved in fugu, frog, chicken, dog and monkey which preserve orthologs of *SHOX* (*Shox*), as well as in opossum which is likely to preserve *Shox*, and were absent in mouse which lack *Shox* (Ensemble Genome Browser, http://ensembl.org/; Fig. 4). Next, MLPA and CGH were performed on the parental samples. The ~46 and ~500 kb deletions were detected in the mother and father, respectively (Figs. 2 and 3A). Thus, the infant was diagnosed as being compound heterozygous for a maternally inherited ~46 kb deletion on the X chromosome and a paternally inherited ~500 kb deletion on the Y chromosome. The results of MLPA and CGH were confirmed by fluorescence in situ hybridization (FISH). FISH probes for *SHOX* exons 3–5 (probe A) and for a region ~320 kb downstream of *SHOX* (probe B) were generated by PCR using primers 5′-CAGCTCTTCCTCAAATTCTTTCC-3′ and 5′-GTGTCTGTCCCATCTCTGGTATC-3′, and 5′-ATAGTG-CATGGGTATCAGAGGTC-3′ and 5′-GGAAAAAGAGTGGGT-

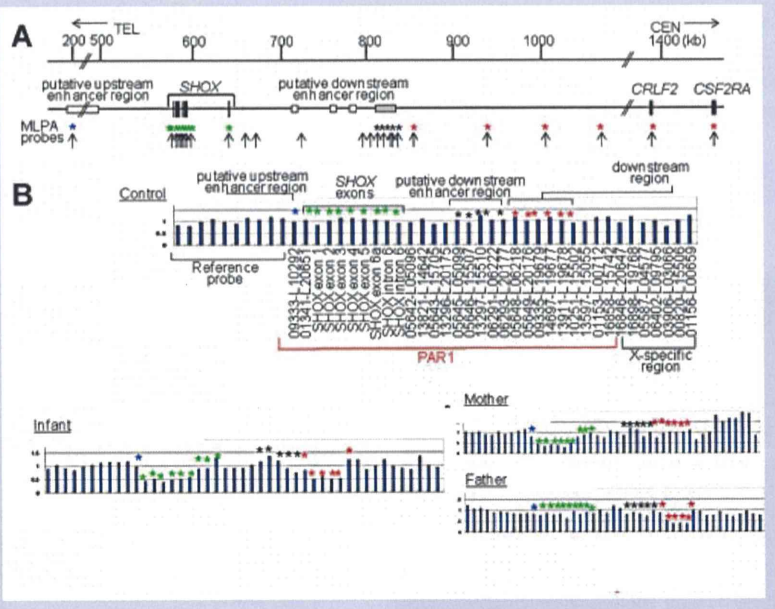

FIG. 2. Multiplex ligation-dependent probe amplification (MLPA) analysis. A: Schematic representation of the short arm pseudoautosomal region (PAR1). The upper horizontal line indicates the physical distance from the Xp/Yp telomere. Genomic positions refer to the Human Genome (hg 19; NCBI Build 37). The black boxes indicate exons of *SHOX*, *CRLF2*, and *CSF2RA* (not all exons are shown). The white box denotes the putative upstream and downstream enhancer regions (elements) of *SHOX* identified in previous studies [Sabherwal et al., 2007; Benito-Sanz et al., 2012a,b]. The gray box indicates putative downstream enhancer elements that exert enhancer activities in the developing chicken limb [Sabherwal et al., 2007]. Vertical arrows indicate genomic positions of MLPA probes; green asterisks indicate probes for *SHOX* exons, blue and black asterisks indicate probes for the putative upstream and downstream enhancer regions respectively, and red asterisks depict probes for the genomic region between the putative downstream enhancer region and *CSF2RA*. TEL, telomere; CEN, centromere. B: Representative results of MLPA. The asterisks indicate the same probes shown in Fig. 2A. The sample data were normalized to a male sample. Decreased peak heights suggest heterozygous deletions. The infant has two deletions; one involving the upstream region and exons 1–5 of *SHOX*, and the other in the downstream region. The mother and father are heterozygous for the deletions.

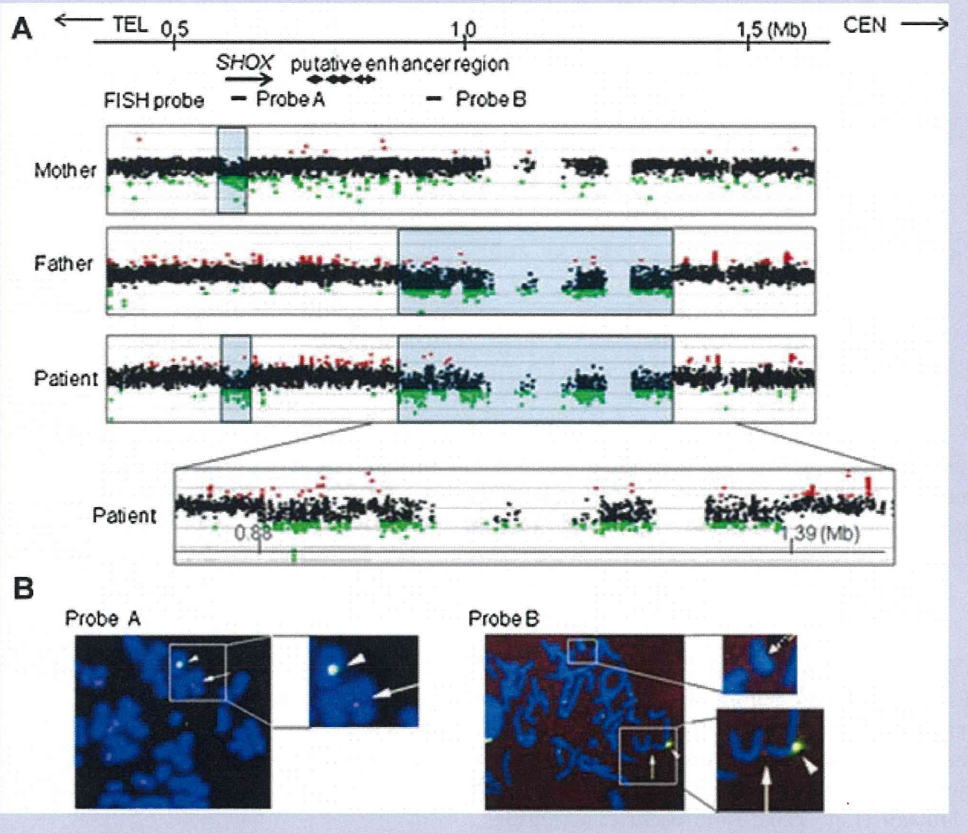

FIG. 3. Comparative genomic hybridization (CGH) and fluorescence in situ hybridization (FISH) analyses. A: CGH analysis in the infant and his parents. The upper horizontal line indicates physical distance from the Xp/Yp telomere. The genomic position of *SHOX*, the putative downstream enhancer elements, and FISH probes are shown. The black, red, and green dots denote signals indicative of the normal, increased (>+0.5), and decreased (<−0.8) copy numbers, respectively. The blue-shaded boxes indicate deleted regions. B: FISH analyses in the infant. Red signals (arrows) indicate probe A for *SHOX* exons 1–3 and probe B for the *SHOX* downstream region, and green signals (arrow heads) depict *DXZ1* control probes on the X chromosome. Probe A detects a signal on the Y chromosome but not on the X chromosome. Probe B detects a signal on the X chromosome but not on the Y chromosome (a dotted arrow).

CAGAACTT-3′, respectively. In the infant, probe A detected only one signal on the Y chromosome and probe B detected only one signal on the X chromosome (Fig. 3B).

We attempted to obtain a DNA sample from the twin brother, because he was predicted to carry the same Y chromosomal deletion as the infant. However, the sample was not available for genetic analysis.

DISCUSSION

We identified compound heterozygous deletions in PAR1 in a male infant. These deletions have not been described previously. The deletion on the X chromosome included most of the coding exons of *SHOX*, and therefore appears to result in complete loss-of-function of the *SHOX* allele. Consistent with this, the mother heterozygous for the same deletion manifested typical clinical features of LWD. In contrast, the deletion on the Y chromosome did not affect exons or the known putative enhancer regions of *SHOX*. Furthermore, this deletion included no genes except *CRLF2*, which has not been implicated in skeletal development [Siracusa et al., 2011]. Clinical examinations of the infant revealed mesomelic short stature and obvious skeletal changes that are more consistent with LMD than with LWD [Fukami et al., 2005; Binder, 2011; Ambrosetti et al., 2013].

Two possible explanations can be made for these results. First, the Y chromosomal deletion in the infant may encompass a hitherto unidentified *cis*-regulatory element of *SHOX*. Recent studies have indicated that several genes such as *SOX9* and *LHX3* have multiple *cis*-acting modules widely distributed around the coding exons [Gordon et al., 2009; Mullen et al., 2012]. Thus, it is possible that coordinated action of multiple regulatory elements is required for adequate *SHOX* expression in the developing limb bud, and that one of such elements is located within the ~500 kb region >300 kb apart from the coding region. Indeed, the Y chromosomal deletion in the infant harbored several CNEs that are well conserved among various species with *SHOX* orthologs.

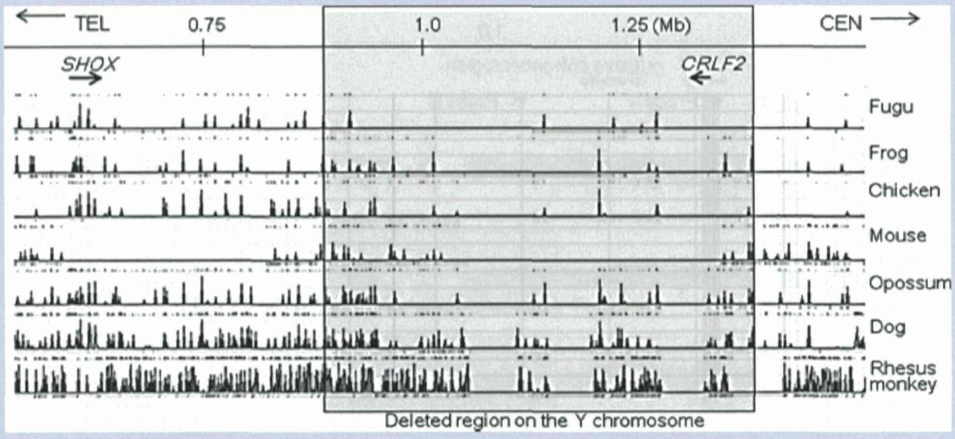

FIG. 4. Conservation analysis in the short arm pseudoautosomal region of the sex chromosomes (PAR1). The deleted region on the Y chromosome (shaded in gray) contains several non-coding elements that are well conserved in species which preserve *SHOX* orthologs (fugu, frog, chicken, dog, and monkey, and possibly opossum as well) and absent in mouse which lacks an *SHOX* ortholog.

One of the CNEs in the deletion may be a distal enhancer of *SHOX/Shox*, because CNEs in the human genome frequently exert enhancer activity [Pennacchio et al., 2006]. In this regard, it is noteworthy that the skeletal features of this infant are milder than those of previously reported patients with *SHOX* nullizygosity [Zinn et al., 2002; Fukami et al., 2005; Ambrosetti et al., 2013]; the infant showed no short stature or rhizomelia at birth. Furthermore, the father with the same Y chromosomal deletion manifested no skeletal abnormalities, and the twin brother with possible Y chromosomal deletion showed only mild proportionate short stature. These results can be explained by assuming that deletions involving only the putative enhancer regions exert a relatively mild effect on skeletal growth compared to mutations/deletions affecting the coding exons. Consistent with this, relatively mild LWD phenotypes have been observed in patients with heterozygous downstream deletions [Rosilio et al., 2012], and mild LMD phenotype has been described in a patient with compound heterozygous deletions for *SHOX* exons and the putative downstream enhancer region [Fukami et al., 2005]. Alternatively, *cis*-regulatory deletions may be associated with broad phenotypic variation compared to exonic deletions/mutations, because Chen et al. [2009] have described profound phenotypes in patients with enhancer deletions.

Second, the phenotype of the infant may be explained as an extremely severe manifestation of LWD. If this is the case, the Y chromosomal deletion would be a functionally neutral copy-number variation. The absence of skeletal changes in the father with the Y chromosomal deletion supports this notion. In this regard, previous studies have indicated that phenotypic severities of *SHOX* haploinsufficiency are variable and likely to be affected by multiple factors [Binder et al., 2004; Binder, 2011]. Thus, some genetic or environmental factors may have enhanced the abnormal skeletal formation of this infant with a maternally derived *SHOX* intragenic deletion.

In summary, we identified hitherto unreported deletions in PAR1 in a Japanese infant with a mild LMD phenotype. Further studies will clarify the presence or absence of a novel downstream enhancer of *SHOX* in the genomic region ~300 to ~800 kb from the start codon.

ACKNOWLEDGMENTS

This work was supported by grants from the following: the Ministry of Health, Labor and Welfare, the Ministry of Education, Culture, Sports, Science and Technology, the National Center for Child Health and Development, the Takeda Science Foundation, and Daiichi-Sankyo Foundation of Life Science.

REFERENCES

Ambrosetti F, Palicelli A, Bulfamante G, Rivasi F. 2013. Langer mesomelic dysplasia in early fetuses: Two cases and a literature review. Fetal Pediatr Pathol [Epub ahead of print].

Belin V, Cusin V, Viot G, Girlich D, Toutain A, Moncla A, Vekemans M, Le Merrer M, Munnich A, Cormier-Daire V. 1998. SHOX mutations in dyschondrosteosis (Leri–Weill syndrome). Nat Genet 19:67–69.

Benito-Sanz S, Thomas NS, Huber C, Gorbenko del Blanco D, Aza-Carmona M, Crolla JA, Maloney V, Rappold G, Argente J, Campos-Barros A, Cormier-Daire V, Heath KE. 2005. A novel class of pseudoautosomal region 1 deletions downstream of SHOX is associated with Leri–Weill dyschondrosteosis. Am J Hum Genet 77:533–544.

Benito-Sanz S, Barroso E, Heine-Suñer D, Hisado-Oliva A, Romanelli V, Rosell J, Aragones A, Caimari M, Argente J, Ross JL, Zinn AR, Gracia R, Lapunzina P, Campos-Barros A, Heath KE. 2011. Clinical and molecular evaluation of SHOX/PAR1 duplications in Leri–Weill dyschondrosteosis (LWD) and idiopathic short stature (ISS). J Clin Endocrinol Metab 96: E404–E412.

Benito-Sanz S, Aza-Carmona M, Rodríguez-Estevez A, Rica-Etxebarria I, Gracia R, Campos-Barros A, Heath KE. 2012a. Identification of the first PAR1 deletion encompassing upsream SHOX enhancers in a family with idiopathic short stature. Eur J Hum Genet 20:125–127.

Benito-Sanz S, Royo JL, Barroso E, Paumard-Hernández B, Barreda-Bonis AC, Liu P, Gracia R, Lupski JR, Campos-Barros Á, Gómez-Skarmeta JL, Heath KE. 2012b. Identification of the first recurrent PAR1 deletion in Léri–Weill dyschondrosteosis and idiopathic short stature reveals the presence of a novel SHOX enhancer. J Med Genet 49:442–450.

Bertorelli R, Capone L, Ambrosetti F, Garavelli L, Varriale L, Mazza V, Stanghellini I, Percesepe A, Forabosco A. 2007. The homozygous deletion of the 3′ enhancer of the SHOX gene causes Langer mesomelic dysplasia. Clin Genet 72:490–491.

Binder G. 2011. Short stature due to SHOX deficiency: Genotype, phenotype, and therapy. Horm Res Paediatr 75:81–89.

Binder G, Renz A, Martinez A, Keselman A, Hesse V, Riedl SW, Häusler G, Fricke-Otto S, Frisch H, Heinrich JJ, Ranke MB. 2004. SHOX haploinsufficiency and Leri–Weill dyschondrosteosis: Prevalence and growth failure in relation to mutation, sex, and degree of wrist deformity. J Clin Endocrinol Metab 89:4403–4408.

Chen J, Wildhardt G, Zhong Z, Röth R, Weiss B, Steinberger D, Decker J, Blum WF, Rappold G. 2009. Enhancer deletions of the SHOX gene as a frequent cause of short stature: The essential role of a 250 kb downstream regulatory domain. J Med Genet 46:834–839.

Clement-Jones M, Schiller S, Rao E, Blaschke RJ, Zuniga A, Zeller R, Robson SC, Binder G, Glass I, Strachan T, Lindsay S, Rappold GA. 2000. The short stature homeobox gene SHOX is involved in skeletal abnormalities in Turner syndrome. Hum Mol Genet 9:695–702.

Durand C, Bangs F, Signolet J, Decker E, Tickle C, Rappold G. 2010. Enhancer elements upstream of the SHOX gene are active in the developing limb. Eur J Hum Genet 18:527–532.

Fukami M, Okuyama T, Yamamori S, Nishimura G, Ogata T. 2005. Microdeletion in the SHOX 3′ region associated with skeletal phenotypes of Langer mesomelic dysplasia in a 45,X/46,X,r(X) infant and Leri–Weill dyschondrosteosis in her 46, XX mother: Implication for the SHOX enhancer. Am J Med Genet Part A 137A:72–76.

Fukami M, Kato F, Tajima T, Yokoya S, Ogata T. 2006. Transactivation function of an approximately 800-bp evolutionarily conserved sequence at the SHOX 3′ region: Implication for the downstream enhancer. Am J Hum Genet 78:167–170.

Fukami M, Dateki S, Kato F, Hasegawa Y, Mochizuki H, Horikawa R, Ogata T. 2008. Identification and characterization of cryptic SHOX intragenic deletions in three Japanese patients with Léri–Weill dyschondrosteosis. J Hum Genet 53:454–459.

Gordon CT, Tan TY, Benko S, Fitzpatrick D, Lyonnet S, Farlie PG. 2009. Long-range regulation at the SOX9 locus in development and disease. J Med Genet 46:649–656.

Mullen RD, Park S, Rhodes SJ. 2012. A distal modular enhancer complex acts to control pituitary- and nervous system-specific expression of the LHX3 regulatory gene. Mol Endocrinol 26:308–319.

Ogata T, Matsuo N, Nishimura G. 2001. SHOX haploinsufficiency and overdosage: Impact of gonadal function status. J Med Genet 38: 1–6.

Pennacchio LA, Ahituv N, Moses AM, Prabhakar S, Nobrega MA, Shoukry M, Minovitsky S, Dubchak I, Holt A, Lewis KD, Plajzer-Frick I, Akiyama J, De Val S, Afzal V, Black BL, Couronne O, Eisen MB, Visel A, Rubin EM. 2006. In vivo enhancer analysis of human conserved non-coding sequences. Nature 23:499–502.

Rao E, Weiss B, Fukami M, Rump A, Niesler B, Mertz A, Muroya K, Binder G, Kirsch S, Winkelmann M, Nordsiek G, Heinrich U, Breuning MH, Ranke MB, Rosenthal A, Ogata T, Rappold GA. 1997. Pseudoautosomal deletions encompassing a novel homeobox gene cause growth failure inidiopathic short stature and Turner syndrome. Nat Genet 16:54–63.

Rosilio M, Huber-Lequesne C, Sapin H, Carel JC, Blum WF, Cormier-Daire V. 2012. Genotypes and phenotypes of children with SHOX deficiency in France. J Clin Endocrinol Metab 97:E1257–E1265.

Sabherwal N, Bangs F, Röth R, Weiss B, Jants K, Tiecke E, Hinkel GK, Spaich C, Hauffa BP, van der Kamp H, Kapeller J, Tickle C, Rappold G. 2007. Long-range conserved non-coding SHOX sequences regulate expression in developing chicken limb and are associated with short stature phenotypes in human patients. Hum Mol Genet 16:210–222.

Shears DJ, Vassal HJ, Goodman FR, Palmer RW, Reardon W, Superti-Furga A, Scambler PJ, Winter RM. 1998. Mutation and deletion of the pseudoautosomal gene SHOX cause Leri–Weill dyschondrosteosis. Nat Genet 19:70–73.

Siracusa MC, Saenz SA, Hill DA, Kim BS, Headley MB, Doering TA, Wherry EJ, Jessup HK, Siegel LA, Kambayashi T, Dudek EC, Kubo M, Cianferoni A, Spergel JM, Ziegler SF, Comeau MR, Artis D. 2011. TSLP promotes interleukin-3-independent basophil haematopoiesis and type 2 inflammation. Nature 14:229–233.

Zinn AR, Wei F, Zhang L, Elder FF, Scott CI Jr, Marttila P, Ross JL. 2002. Complete SHOX deficiency causes Langer mesomelic dysplasia. Am J Med Genet 110:158–163.

Novel Insights from Clinical Practice

HORMONE RESEARCH IN PÆDIATRICS

Horm Res Paediatr 2014;82:65–71
DOI: 10.1159/000360291

Received: November 20, 2013
Accepted: February 3, 2014
Published online: June 11, 2014

Association between Compound Heterozygous Mutations of *SLC34A3* and Hypercalciuria

Yuki Abe[a] Keisuke Nagasaki[b, c] Toru Watanabe[a] Tokinari Abe[a] Maki Fukami[c]

[a]Department of Pediatrics, Niigata City General Hospital, [b]Division of Pediatrics, Department of Homeostatic Regulation and Development, Niigata University Graduate School of Medical and Dental Sciences, Niigata, and [c]Department of Molecular Endocrinology, National Research Institute for Child Health and Development, Tokyo, Japan

Established Facts

- Patients with biallelic mutations in *SLC34A3* show clinical features of hereditary hypophosphatemic rickets with hypercalciuria.

Novel Insights

- Biallelic mutations in *SLC34A3* can cause hypercalciuria not accompanied by rickets.
- Mutation of *SLC34A3* should be considered in patients with hypercalciuria of unknown etiology, even in the absence of skeletal lesions in the patients themselves or their family members.

Key Words

Compound heterozygous *SLC34A3* mutations · Hereditary hypophosphatemic rickets with hypercalciuria · Hypercalciuria · Hypophosphatemic rickets · NaPi-IIc

Abstract

Background: Mutations in *SLC34A3* have been shown to cause hereditary hypophosphatemic rickets with hypercalciuria (HHRH). Patients with compound heterozygous or homozygous mutations develop skeletal lesions in addition to hypercalciuria, hypophosphatemia and/or elevated 1,25-dihydroxy vitamin D [1,25-$(OH)_2$D] levels. Here, we report a case of hypercalciuria without skeletal lesions in a patient with compound heterozygous mutations of *SLC34A3*. ***Case Presentation:*** A 3-year-old girl presented with microscopic hematuria. Laboratory data revealed elevated 1,25-$(OH)_2$D levels and serum calcium, reduced serum inorganic phosphorus and hypercalciuria. In addition, the ratio of maximal rate of renal tubular reabsorption of phosphate to glomerular filtration rate was reduced. Abdominal ultrasound revealed bilateral nephrocalcinosis. These data were consistent with HHRH, but the patient had no clinical features of rickets or any family history of skeletal disease. Genetic analysis revealed compound heterozygous mutations of c.175+1 G>A and c.1234 C>T in *SLC34A3*. ***Conclusions:*** This is the report of a patient with compound heterozygous mutations of *SLC34A3* and normal skeletal features. Biallelic mutations in *SLC34A3* can thus be associated with hypercalciuria not accompanied by rickets. Orally administered inorganic phosphate is predicted to improve symptoms in these patients, hence screening for *SLC34A3* mutations should be considered in patients with hypercalciuria of unknown etiology.

KARGER

E-Mail karger@karger.com
www.karger.com/hrp

1663–2818/14/0821–0065$39.50/0

Yuki Abe, MD, PhD
Department of Pediatrics
Niigata City General Hospital
463-7 Shumoku, Chuo-ku, Niigata 950-1197 (Japan)
E-Mail y-abe@hosp.niigata.niigata.jp

Introduction

Hereditary hypophosphatemic rickets with hypercalciuria (HHRH; MIM #241530) is a rare autosomal recessive metabolic disorder, first described by Tieder et al. [1] in a large Bedouin tribe in 1985. It becomes symptomatic in early childhood and is characterized by rickets, short stature, decreased renal phosphorus reabsorption and hypercalciuria.

In 2006, Bergwitz et al. [2], Lorenz-Depiereux et al. [3] and Ichikawa et al. [4] demonstrated that mutations in *SLC34A3*, the gene that encodes the renal type 2c sodium-phosphate cotransporter (NaPi-IIc), contribute to the pathophysiology of HHRH. NaPi-IIc is expressed at the renal brush border membrane of proximal tubules. It has sodium-dependent inorganic phosphate cotransport activity and mediates renal phosphate reabsorption [5].

Patients with heterozygous mutations of *SLC34A3* show either no symptoms or hypercalciuria, often associated with mild hypophosphatemia and/or elevated 1,25-dihydroxy vitamin D [1,25-$(OH)_2$D], but no skeletal lesions. Conversely, patients with compound heterozygous or homozygous mutations develop rickets in addition to these symptoms. Indeed, biallelic mutations of the *SLC34A3* gene have been identified in HHRH patients.

Here, we report the description of a patient with compound heterozygous mutations of *SLC34A3* but without skeletal lesions.

Case Report

The patient, a 3-year-old girl, presented with microscopic hematuria and pyuria, detected on routine physical examination. She was born healthy and had had no medical problems. Her parents were non-consanguineous Japanese individuals with no medical problems. Her family history was significant for a lack of short stature, electrolyte disorders, or skeletal diseases. She had no family history of renal disorders, except her maternal grandfather who developed renal stones in late adulthood.

Physical examination revealed a height of 93.8 cm [–0.91 standard deviation (SD)] and a weight of 15.3 kg (+0.53 SD), based on the standard anthropometric data of Japanese children. No skeletal abnormalities, including genu varum, were observed. Her chest and abdomen were unremarkable. Her vital signs were normal for her age with the exception of a high daily urine volume (4,200 ml/m^2/day on average).

Laboratory data on presentation revealed the following: sodium 140 mEq/l, potassium 4.1 mEq/l, chlorine 103 mEq/l, calcium 11.4 (reference value: 9.0–10.2) mg/dl, inorganic phosphorus 4.5 (4.5–6.5) mg/dl, serum alkaline phosphatase 808 (334–897) IU/l, blood urea nitrogen 14.8 mg/dl, and creatinine 0.45 mg/dl. Venous blood gas analysis showed a pH of 7.383, PCO_2 of 42.8 mm Hg, PO_2 of 41.7 mm Hg, HCO_3^- of 24.9 mEq/l, base excess of –0.3 mEq/l and SvO_2 of 76.5%. Urinalysis was negative for protein and glucose but positive for occult blood (3+) and leukocyte esterase (2+). Urine-specific gravity was low at 1.005. Urine sediment revealed 1–4 RBCs/HPF, 5–9 WBCs/HPF. No urinary casts were detected. Urine β_2-microglobulin was 0.07 (<0.15) mg/l and the calcium/creatinine ratio was 0.40 (<0.42). Bilateral nephrocalcinosis was detected on abdominal ultrasound. The hypercalcemia and nephrocalcinosis led us to evaluate 24-hour urine calcium excretion and calciotropic hormones. Her urine calcium excretion was elevated up to 11 (<4) mg/kg/day. The lower limit of serum intact parathyroid hormone (PTH) was at 10 (10–65) pg/ml. Serum 25-hydroxy vitamin D (25-OHD) was normal at 27 (7–40) ng/ml and 1,25-$(OH)_2$D was elevated at 71.7 (20–60) pg/ml. The serum calcium re-examined in the morning fasting was slightly elevated at 11.0 mg/dl and concomitant inorganic phosphorus was reduced at 2.5 mg/dl. Because of low fasting inorganic phosphorus levels, we checked the ratio of maximal rate of renal tubular reabsorption of phosphate to glomerular filtration rate (TmP/GFR) and found it reduced at 2.4 (4.7–5.1) mg/dl. Plasma arginine vasopressin levels were elevated to 23.2 pg/ml, while concomitant plasma and urine osmolality was 285 and 299 mOsm/kg, respectively. The urine osmolality showed almost no reaction to the exogenous vasopressin (307 mOsm/kg 3 h after administration), indicating the reduced renal sensitivity to antidiuretic hormone probably due to hypercalcemia.

These findings were similar to the biochemical features of HHRH. However, the patient lacked any physical evidence of skeletal abnormalities. Knee X-rays and MRI did not demonstrate evidence of rickets (fig. 1). Discovery A dual-energy X-ray absorptiometry (Hologic, Inc., Bedford, Mass., USA) revealed a normal bone density of 0.453 g/cm^2 (Z-score: –1.1).

The patient's parents and younger sibling exhibited normal levels of serum calcium and inorganic phosphorus, normal urinary calcium/creatinine ratios and normal TmP/GFR. Furthermore, they had neither skeletal abnormalities nor hematuria and abdominal ultrasounds showed no renal stones (table 1).

Genetic Analysis

Genetic analyses of the patient, her parents and her younger sibling were performed after written informed consent was obtained from the parents, using forms approved by the Institutional Review Board of the National Research Institute for Child Health and Development. All coding exons and flanking introns of *SCL34A3* (MIM *609826) were analyzed by PCR-based screening. PCR products were then directly sequenced on the CEQ 8000 autosequencer (Beckman Coulter, Fullerton, Calif., USA).

Direct sequencing results are shown in figure 2. The patient was found to have compound heterozygous mutations of *SCL34A3* consisting of c.175+1 G>A (c.IVS3+1 G>A) on the maternal allele and c.1234 C>T, a missense mutation substituting tryptophan (TGG) for arginine (CGG) at codon 412 (Arg412→Trp: R412W), on the paternal allele (RefSeq Accessions NG_017008.1 for genomic contig, NM_080877.1 for cDNA sequence and NP_543153 for protein sequence). The mutation c.1234 C>T was described as a single nucleotide polymorphism (SNP) in the database (rs373242362). The parents were heterozygous for the respective mutated and wild-type allele and the younger sibling was homozygous for the wild-type allele (table 1).

Fig. 1. Radiograph and MRI of the patient's knee joint. No evidence of rickets was observed.

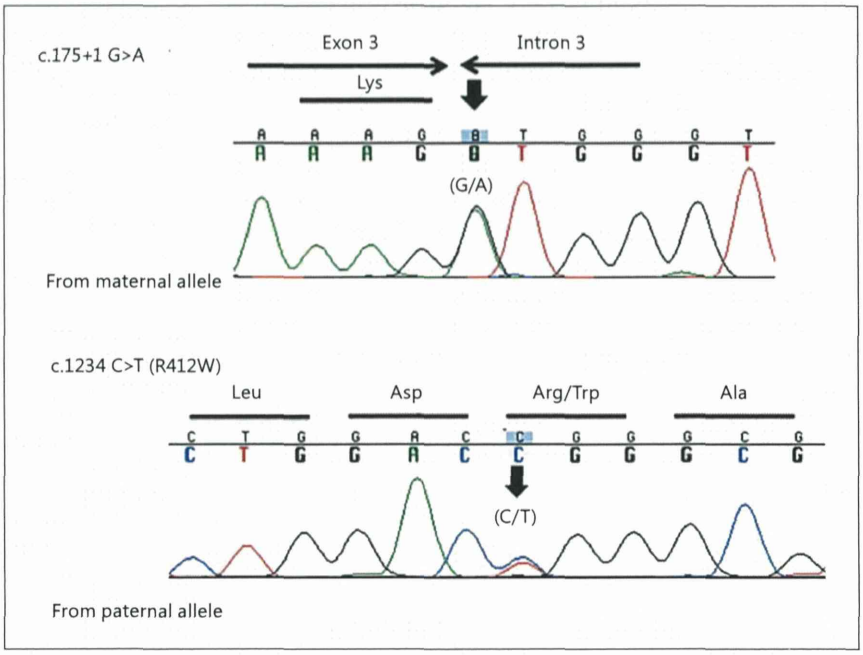

Fig. 2. Direct sequencing of *SLC34A3*. The patient was found to have compound heterozygous mutations of *SCL34A3*. The c.175+1 G>A (c.IVS3+1 G>A) mutation of the maternal allele occurs at the first nucleotide in the donor splice site of intron 3, and is predicted to cause a splicing error. The c.1234 C>T mutation of the paternal allele is a missense mutation in which tryptophan is substituted for arginine at codon 412 (R412W).

Table 1. Laboratory data and clinical manifestations of first-degree relatives

	Father	Mother	Sibling
Ca, mg/dl	9.6 (8.2–9.9)	9.2 (8.2–9.9)	10.1 (9.0–10.2)
Pi, mg/dl	2.9 (2.4–4.5)	3.4 (2.4–4.5)	5.6 (4.5–6.5)
Urine-Ca/Urine-Cre	0.04 (<0.20)	0.03 (<0.20)	0.02 (<0.60)
TmP/GFR	2.4 (2.6–4.4)	2.8 (2.6–4.4)	5.4 (4.7–5.7)
Hematuria	–	–	–
Renal calcification	–	–	not examined
Bone abnormality	–	–	–
c.1234 C>T	+	–	–
c.175+1 G>A	–	+	–

Pi = Inorganic phosphorus; Cre = creatinine; TmP/GFR = ratio of the maximal renal phosphate reabsorption to glomerular filtration rate. Laboratory data were obtained after fasting overnight.

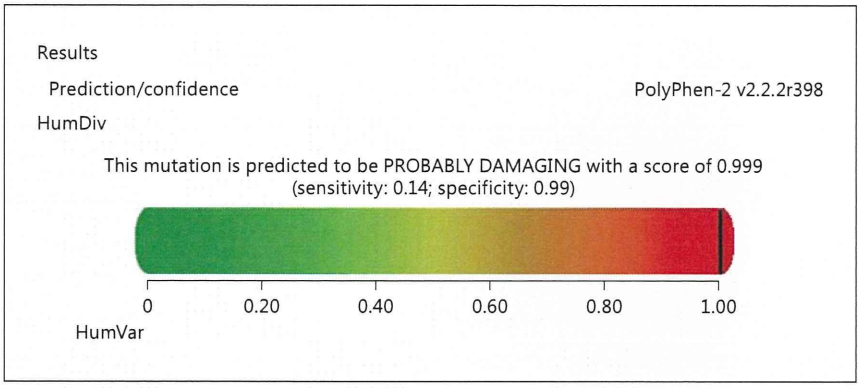

Fig. 3. Report of the mutation R412W (c.1234 C>T) in *SLC34A3* by PolyPhen-2. The mutation was predicted to cause functional damage of NaPi-IIc.

Table 2. Laboratory data at presentation and throughout treatment

	Pretreatment		Posttreatment, weeks							
	1st visit	2nd visit	0	4	12	16	20	28	37	41
Oral phosphate, mg/kg/day		0		30	40		50	60		70
Ca (9.0–10.2), mg/dl	11.4	11.0	11.0	10.4	10.4	11.0	10.6	10.6	10.3	10.1
Pi (4.5–6.5), mg/dl	4.5	2.5	4.1	4.0	4.4	5.4	5.0	5.7	4.4	4.9
Intact PTH (10–65), pg/ml	10	NE	5	6	10	9	9	15	13	20
1,25-$(OH)_2$D (20–60), ng/ml	71.7	NE	127	74.8	98.4	83.0	61.0	57.2	59.9	49.4
25-OHD (7–40), pg/ml	27	NE	24	39	36	44	41	25	26	21
Urine-Ca/urine-Cre (<0.42)	0.40	0.38	0.78	0.12	0.18	0.22	0.31	0.24	0.23	0.22
TmP/GFR (4.7–5.1)	3.8	2.4	3.3	2.9	3.1	4.4	3.5	4.3	2.6	3.4
ALP (334–897), IU/l	808	NE	943	683	597	651	646	542	597	655
BAP (31–152), U/l	NE	NE	98.6	68.6	55.2	65.7	66.6	54.5	58.0	72.1
FGF23 (10–50), pg/ml	NE	NE	<10	<10	<10	11	12	13	20	23
Serum-BUN (8.0–19.7), mg/dl	14.8	10.5	13.6	10.5	9.8	10.8	15.0	15.4	13.2	13.9
Serum-Cre (0.40–0.80), mg/dl	0.45	0.36	0.39	0.43	0.43	0.41	0.42	0.42	0.43	0.39
eGFR (>90), ml/min/1.73 m^2	251	320	293	242	242	255	249	249	242	270
Urine occult blood	2+	3+	3+	2+	2+	2+	2+	2+	2+	1+
Urine leukocyte elastase	2+	3+	3+	3+	3+	3+	3+	2+	2+	2+

ALP = Alkaline phosphatase; BAP = bone alkaline phosphatase; BUN = blood urea nitrogen; NE = not examined. Other abbreviations as in table 1.

In silico Analysis

The c.1234 C>T mutation in *SLC34A3* was submitted to in silico analysis. The results exhibited that this mutation was predicted to cause functional damage (PolyPhen-2 [6]: damage score 0.999, sensitivity 0.14, specificity 0.99 (fig. 3) and SIFT [7]: substitution at position 412 from R to W is predicted to affect protein function with a score of 0.00, median sequence conservation: 2.46, sequences represented at this position: 94).

Clinical Course

The patient's nephrocalcinosis was thought to be due to a functional loss of NaPi-IIc, similar to the pathophysiology of HHRH. Oral administration of inorganic phosphate (30 mg/kg/day, q.i.d.) was initiated. Although the urine calcium/creatinine ratio immediately decreased to 0.12, the serum inorganic phosphorus and intact PTH levels remained low at 4.0 mg/dl and 6 pg/ml, respectively, and the serum 1,25-$(OH)_2$D levels remained high. The dose was thus raised to 50–60 mg/kg/day. At this dose, 1,25-$(OH)_2$D and fibroblast growth factor 23 (FGF23) (Kainos Laboratories, Tokyo, Japan) levels normalized. Serum alkaline phosphatase and bone-specific alkaline phosphatase levels decreased. Her renal function remained normal before and during the course of therapy (table 2). An abdominal ultrasound performed 3 months after showed no significant changes. The dose of oral inorganic phosphate was increased to 70 mg/kg/day based on serum inorganic phosphorus and 1,25-$(OH)_2$D levels. The abnormal urine sedi-

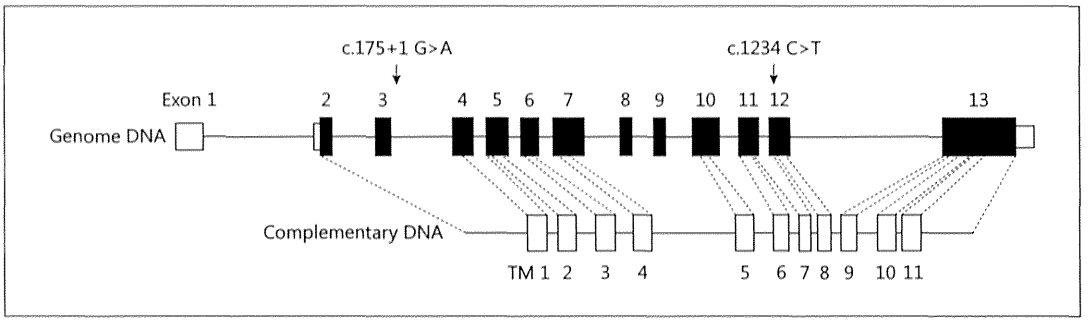

Fig. 4. Scheme of human NaPi-IIc DNA and the positions of mutations in our case. The genome DNA consists of 13 exons (open and black squares show untranslated and translated regions, respectively) and 12 introns. The complementary DNA has 11 transmembrane (TM) domains (open squares). The source of transmembrane domains was obtained from Ensembl [9].

ment persisted for several months (urine RBCs and WBCs both peaked at 50–99/HPF) and then almost normalized after 10 months of treatment (urine RBCs and WBCs recovered to 5–9/HPF and 10–19/HPF, respectively).

Discussion

Mutations in *SLC34A3* cause the functional loss of NaPi-IIc, a molecule that plays a critical role in the renal conservation of phosphorus. We detected two mutations of this gene. The first, c.175+1 G>A, was found on the maternal allele. This mutation changes the first nucleotide of the donor splice site of intron 3. The 'GT' dinucleotide is commonly found at 5′ splice sites, hence this mutation likely results in a splicing error [8]. The second mutation, c.1234 C>T, was found on the paternal allele. It is a missense mutation, resulting in the substitution of tryptophan (TGG) for arginine (CGG) at codon 412 in exon 12 (fig. 4). There are many experimentally characterized non-synonymous SNPs (nsSNPs) annotated in the databases. Each nsSNP can either affect its gene products or be neutral in its gene production. However, many of these nsSNPs lack experimental annotations of their functional impacts. The mutation c.1234 C>T (R412W) was described as a SNP in the database. Though there was no experimental annotation about whether its function was neutral or deteriorated, this variant was considered very rare (T = 2/C = 12986) [10] and we could not find a similar variant either in 100 control alleles or in the Japanese exome database [11]. Moreover, R412 is well conserved among species. Because it is highly improbable that such rare variant shows homozygosity or compound heterozygosity with another mutated gene, deteriorating impact of the variant is considered to be hard to become apparent. Rare nsSNPs in general could indeed deteriorate the function of the gene products and cause diseases. Based on these results and in silico analysis, we guessed that c.1234 C>T causes the functional loss of NaPi-IIc.

Functional derangements of NaPi-IIc cause serum phosphorus depletion, 1,25-$(OH)_2$D elevation and renal calcium reabsorption, leading to hypercalcemia and increased urinary calcium excretion [1, 3]. Phosphorus repletion is predicted to resolve hypercalciuria by reducing serum 1,25-$(OH)_2$D levels. However, Yu et al. [12] reported that serum 1,25-$(OH)_2$D levels remained high after oral inorganic phosphate administration and normalization of urine calcium excretion. In our patient, decrease of the urine calcium/creatinine ratio was observed first at the dose of inorganic phosphate of 30 mg/kg/day, followed by normalization of serum FGF23 levels at the dose of 50 mg/kg/day and 1,25-$(OH)_2$D levels at the dose of 60 mg/kg/day. This finding cannot be explained by the commonly accepted mechanism of hypercalciuria described above.

FGF23 is a serum peptide that regulates serum phosphorus levels. FGF23 reduces renal reabsorption and increases urinary excretion of phosphorus by reducing the expression of the NaPi-IIa and NaPi-IIc cotransporters in proximal renal tubular cells [13]. It also inhibits 1α-hydroxylase, thereby reducing 1,25-$(OH)_2$D production by the kidney [14]. We found that normalization of FGF23 levels preceded normalization of 1,25-$(OH)_2$D levels when the dose of inorganic oral phosphate was raised to 50 mg/kg/day. This finding suggests that FGF23 is downregulated in patients with NaPi-IIc dysfunction,